Sol-gel synthesis and Characterization of Structural and Luminescence Properties of $ZnAl_2O_4$ doped with Mn^{2+} powder phosphor

SV Motloung[1], FB Dejene[*1,3], HC Swart[2], OM Ntwaeaborwa[2]

[1]Department of Physics, University of the Free State (Qwaqwa Campus), Private Bag X13, Phuthaditjhaba, 9866, South Africa

[2]Department of Physics, University of the Free State, P.O. Box 339, Bloemfontein, 9300, South Africa

[*]Corresponding author: Dejenebf@qwa.ufs.ac.za or SwartHC@ufs.ac.za

Abstract. Pure and ultrafine cubic $ZnAl_2O_4$ doped with Mn^{2+} ions were prepared at a low temperature below 80 °C by a sol-gel process. The dopant (Mn^{2+}) concentrations and Zn/catalyst mole ration in a solution were varied. The gel, as prepared and heat-treated powder samples were characterized by thermogravimatric analysis (TGA), Fourier transform infrared analysis (FTIR), X-ray diffraction (XRD), scanning electron microscopy (SEM), electron diffraction spectroscopy (EDS) and photoluminescence (PL). The TGA confirmed that the minimum annealing temperature to obtain pure and single phase $ZnAl_2O_4$ must be above 400 °C in order to remove organic residues. The XRD data revealed that all the heat-treated samples were single phase crystalline structures and the estimated crystaline sizes were in the range of 3-65 nm in diameter. The surface morphology of the phosphors was influenced by the Mn dopant concentration and Zn/catalyst mole ratio in the solution. EDS confirmed the presence of the expected elements. PL spectra indicated that the position of the peak changed depending on the Mn content and 0.25 mol% had the highest intensity centred at 510 nm. The mole ratio of Zn/catalyst = 1.33 had the highest intensity centred at 435 nm.

1. Introduction

Zinc aluminate ($ZnAl_2O_4$) has been attracting considerable attention since it may be used as a UV-transparent conductor, sensors, dielectric material, high temperature ceramic, catalyst and catalyst support [1-3]. Apart from these properties, $ZnAl_2O_4$ is also being considered for photo-electronic device on account of its wide-bandgap nature estimated to be about 3.8 eV [4,5]. Nanostructured materials have attracted considerable interest among researchers due to their remarkable physical properties such as; decreases size, increases surface-to-volume ratio and novel morphologies. The luminescence property of phosphor is known strongly to dependent on the particle size, crystal structure, and uniform distribution of activators in the host lattice [4,5,6]. In recent years, numerous methods of fabrication of $ZnAl_2O_4$ such as solid state reaction [7,8], co-precipitation method [9,10], hydrothermal [11], combustion [6,12,13] and sol-gel [4,14] have been developed. Compared with the traditional techniques, sol-gel route is a versatile and attractive technique for the fabrication of nanocrystalline powders because of its advantage of producing pure and ultrafine powders at a very low temperature [4,15]. However, there are scarce works reported on sol-gel synthesis of $ZnAl_2O_4$ doped with Mn in literature to date. On the other hand, Zn/catalyst molar ratio as a function of luminescence, to the best of our knowledge, has not been attempted so far. Thus, in this work, an attempt is being made to report on the single-phase $ZnAl_2O_4$ nanopowders doped with Mn^{2+} at the varying molar ratio of Zn/Mn and Zn/catalyst in a solution.

2. Experiment

The precursor of $ZnAl_2O_4$ was prepared by dissolving $Zn(NO_3)_2.6H_2O$ (98%) and $Al(NO_3)_3.9H_2O$ (98.5%) in deionized water. The sols stoichiometric ratio was set to obey the 2:1 molar ration of Zn/Al. Citric acid, $C_8H_8O_7.H_2O$ (99%), was used as a catalyst. For the first part of the experiment, the molar ration of Zn/catalyst was kept constant at 1:3. To investigate the luminescence dependence on the dopant concentration, proper amounts of $MnNO_3.xH_2O$ (99.99%) was added for doping, and the molar ratio of Mn/Zn was varied between 0.05 and 3 mol%. The concentration of the dopant that gave the highest brightness (from the first part) was kept constant for the second part of the experiment and the Zn/catalyst molar ration was varied between 0.08 and 1.33 moles to investigate the luminescence

as a function of catalyst concentration. Each solution was heated below 80^0C with constant stirring on a magnetic stirrer for a few hours until gelation had taken place following a chemical reaction. The transparent gel was achieved and heated at a temperature of 150 ^{0}C in an oven for powders synthesis. The powders samples were ground and subsequently heat-treated at 700 ^{0}C for an hour. Thermogravimetric analysis of the gel was carried out using a Perkin Elmer TGA7 in the temperature range of 30-745 ^{0}C at a heating rate of 10 ^{0}C /min under an air flux. The stretching mode frequencies were determined using a Perkin Elmer Spectrum 100 FTIR spectrometer. The processed samples crystal structures were characterized by powder X-ray diffraction (Bruker AXS Discover diffractometer) with CuKα (1.5418Å) radiation). The surface morphology and elemental composition of the phosphor powder were investigated using a Shimadzu Superscan ZU SSX-550 electrom microscope (SEM) coupled with an energy dispersive X-ray spectroscope (EDS). A photoluminescence system consisting of a 325 nm He-Cd laser, SPEX 1870 0.5 m monochromator and a photomultiplier tube was used to record photoluminescence (PL) spectra.

3. Results and discussion

3.1. Thermogravimatric analysis

The thermal decomposition of the as prepared gel is depicted in figure 1. The variation of the mass of the compound with temperature indicates a strong loss up to 80 ^{0}C due to the release of interlayer water [16]. An event at around 150-200 ^{0}C, is attributed to the formation of the powder hydroxides of zinc and aluminium and expulsion of hydrated water [17]. The last event very close to 300 ^{0}C is credited for the crystallization process and the formation of single phase $ZnAl_2O_4$.

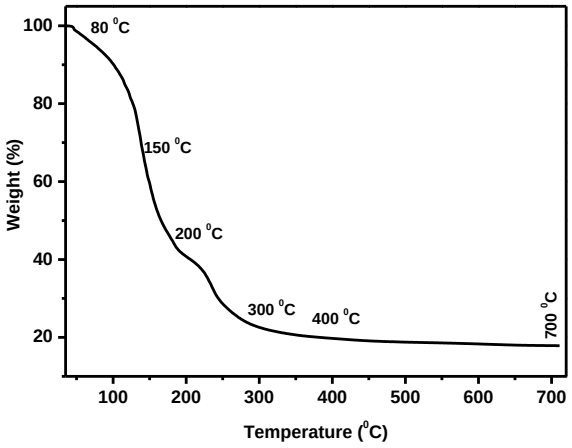

Figure 1. TGA curve of $ZnAl_2O_4$ gel

These results showed that the minimum annealing temperature to obtain pure and single phase $ZnAl_2O_4$ must be above 400 ^{0}C in order to remove organic residues and this is consistent with what was observed in the XRD and FTIR analysis.

3.2. X-ray diffraction

The XRD patterns of the $ZnAl_2O_4$:Mn^{2+} powders dried at 150 ^{0}C in an oven and heat-treated at 700 ^{0}C in a furnace are shown in figure 2. Note that all samples exhibited similar characteristics after annealing at high temperature. This implies that the Mn doping content and Zn/catalyst molar ratio had no significant effects on the structural properties of the product. The intermediary phase obtained when powders are dried at 150 ^{0}C, is attributed to a mixture of aluminium and zinc oxides. This kind of behaviour is certainly due to the incompleteness of the chemical reaction during synthesis. Thus, it

is strongly believed that $ZnAl_2O_4$ was not successfully formed for the first part of the experiment. The estimated particle size reported in this study was calculated by using the Debye-Scherrer formula [18].

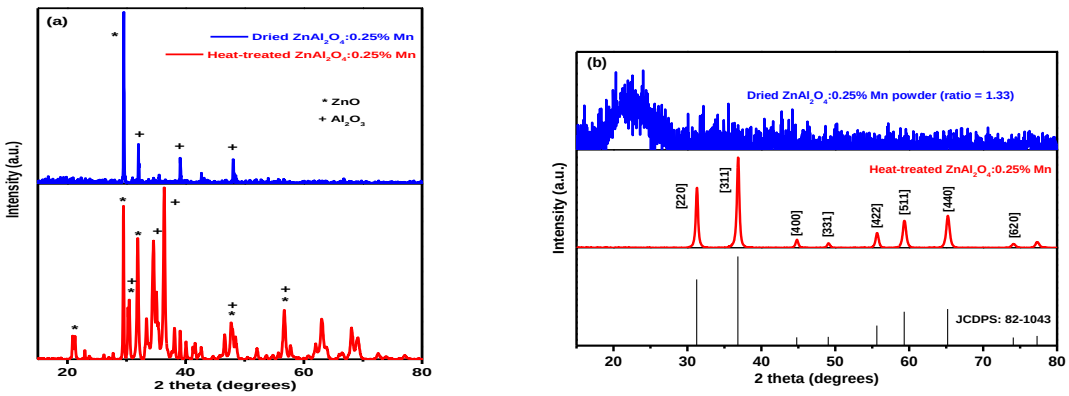

Figure 2. The XRD pattern of Mn^{2+}-doped $ZnAl_2O_4$ nanophosphors for various (a) Mn^{2+}-concentrations and (b) Zn/catalyst mole ratio

In figure 2 (a) the particle size obtained for the dried and heat-treated powders are estimated to be 147 and 62.5 nm respectively. In figure 2 (b), the dried powder is amorphous with small particle size of 3.4 nm and the average particle size of the heat treated powder increases to 46 nm while the structure transforms to the cubic phase. All the diffraction peaks in figure 2 (b) were consistent with the standard data for the cubic $ZnAl_2O_4$ spinel phase (JCDPS: 82-1043). The results clearly reveal that highly crystalline cubic $ZnAl_2O_4$ single phase can be obtained after annealing at 700 ^{0}C.

3.3 SEM

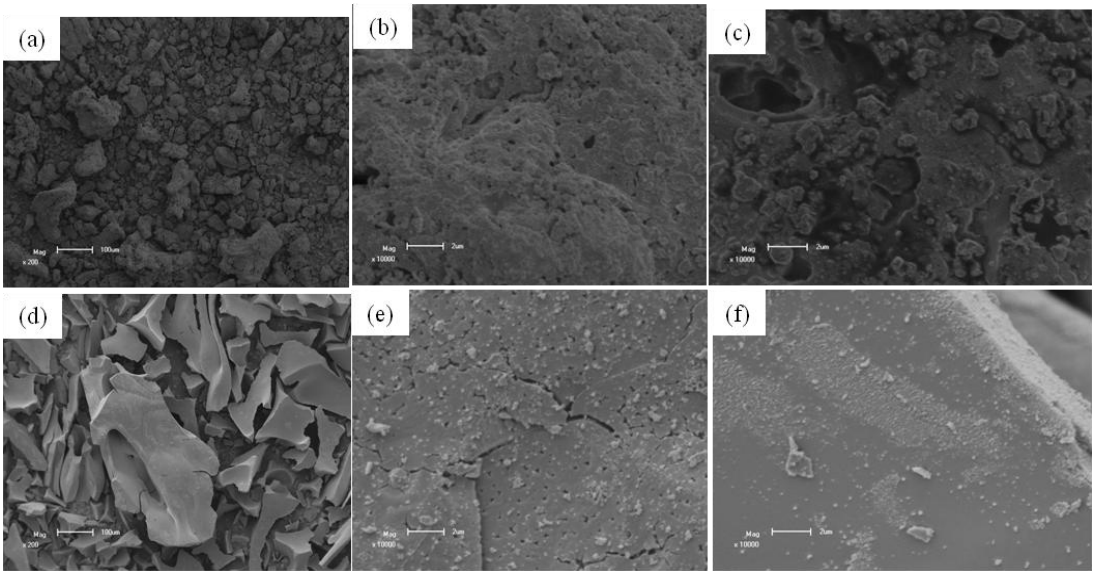

Figure 3. SEM micrographs of the 700 ^{0}C heat-treated nano-powder (a) x200 Magnification of $ZnAl_2O_4$:0.25% Mn (b) x 10000 Magnification of $ZnAl_2O_4$:0.25% Mn, (c) x 10000 Magnification of $ZnAl_2O_4$:1% Mn, (d) x200 Magnification of $ZnAl_2O_4$:0.25% Mn (Zn/catalyst) = 1.33 (e) x 10000 Magnification of $ZnAl_2O_4$:0.25% Mn (Zn/catalyst) = 1.33 and (f) x 10000 Magnification of $ZnAl_2O_4$:0.25% Mn (Zn/catalyst) = 0.11

In figure 3 (a), (b) and (c), the phosphor morphology consists of the granular structures with pores and agglomerated particles. It was found that the degree of porosity increases with the Mn content, which suggests that the dopant content influences the morphology. In figure 3 (e) and (f), the particles consists of spherical particles, which are plate-like structured with small particle embedded (figure 3 (f)). For the lower magnifications (figure 3 (d)) this particles have a flake like morphology. It suggests that the Zn/catalyst mole ratio affects the morphology of the phosphor.

3.4 EDS and FTIR

The FTIR spectra of the $ZnAl_2O_4$:0.25% Mn gel, dried and heat-treated powders are shown in figure 4 (a). The IR spectra of the gel and dried powders indicate the presence of nitrates groups (806, 855, 896 and 1043 cm^{-1}) [20]. The bands at 1588 and 1384 cm^{-1} can be attributed to the OH group in the metal alkoxides present in the gel. It can be seen that similar bands are denoted by 1596 and 1295 cm^{-1} in the dried powder and the bands are slightly compressed compared to the gel and this can be due to the formation of amorphous (see figure 2 (b)) or intimidate phase (see figure 2 (a)) compound prior to the formation of the single phase $ZnAl_2O_4$ [17]. Wide absorption band centred at 3185 (for the dried) and 3290 cm^{-1} (for the gel) corresponds to OH group, which is contributed by the water content [17]. As expected the wide absorption band is more pronounced in the gel than in dried powder. Moreover, the bands at 3185, 3770 and 1596 cm^{-1} can be assigned to the deformation mode of water and vibration mode of carbon containing groups [17,6]. The results show that the amount of water present in the sample reduces with the temperature increase. Generally, there are no bands for the heat-treated/fired samples, which imply that, the pure and ultrafine $ZnAl_2O_4$:0.25% Mn was achieved. The results showed that the bands decreases from gel, dried and heat-treated samples, which suggest that heat-treating has a major effect on destroying some bonds. These results agree with the TGA and XRD results.

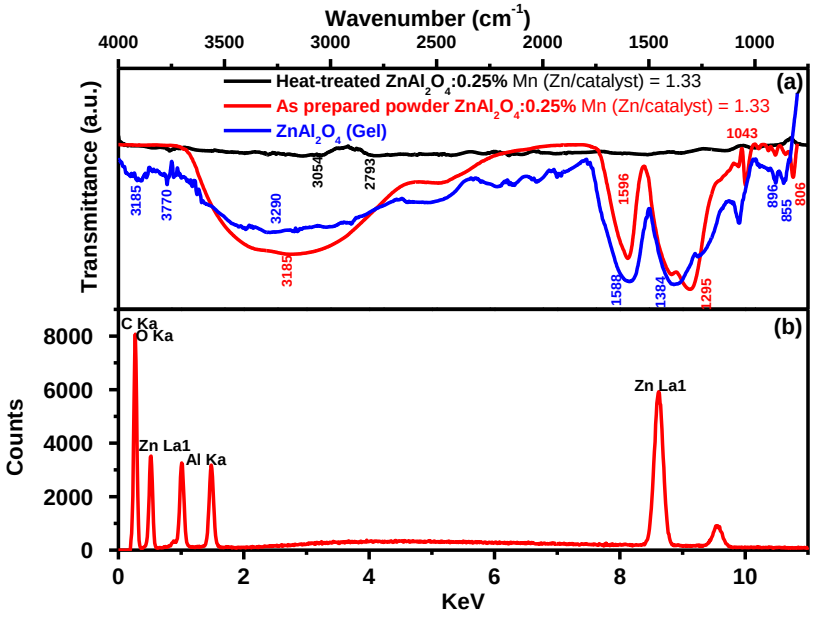

Figure 4. FTIR spectrum of the as prepared, heat treated $ZnAl_2O_4$:0.25% Mn and $ZnAl_2O_4$ gel (a) and the EDS spectrum of $ZnAl_2O_4$:0.25% Mn nanoparticles (b).

The energy dispersive spectrum of the particles is shown in figure 4 (b). The counts corresponding to C is from the double sided carbon tape. The expected elements Zn, Al and O are evidently noticed in a spectrum, suggesting that the nanoparticles are only made up of Zn, Al and O. The presence of the foreign element (Mn) is not detected in a spectrum and this is attributed to the low mol% used for

doping ($ZnAl_2O_4$:0.25% Mn). The existence of C (carbon) is believed to have originated from the double sided carbon tape.

3.5 Photoluminescence analysis

F igure 5 (a) illustrates the dependence of the emission intensity of $ZnAl_2O_4:Mn^{2+}$ as a function of the Mn doping content. The emission spectra of all samples are dominated by broad green emission band centred around 512 nm, which correspond to the typical $^4T_1(^4G)$-$^6A(^6S)$ transition of tetrahedral Mn^{2+} ion [19]. In figure 5 (b) the emission intensity increases with increasing dopant concentration and reaches a maximum at 0.25 mol % of Mn^{2+}. Concentration quenching is observed when the Mn^{2+} concentration was above 0.25 mol%. In figure 5 (c) the red shift of the dominant green emission peak reflects a change in ligand field strength as a result of concentration-dependent exchange interactions between neigh-boring Mn^{2+} ions [21].

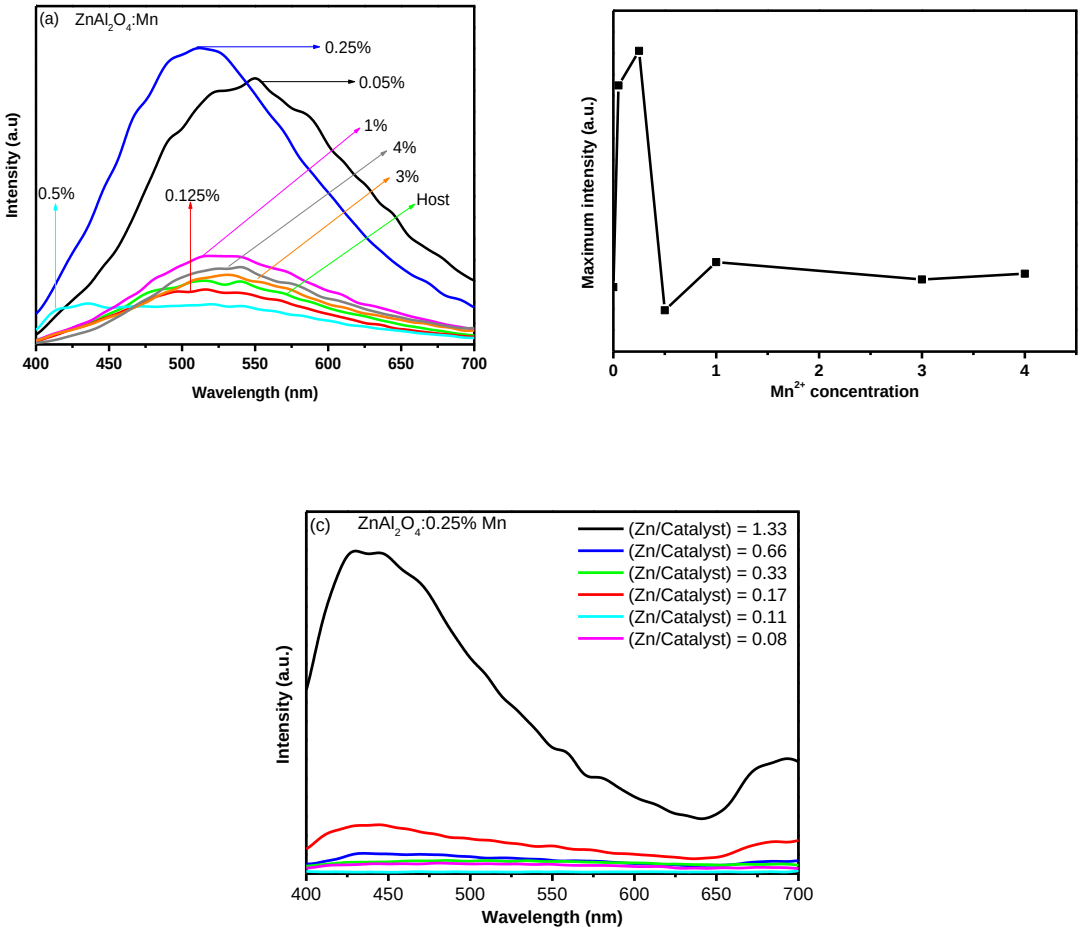

Figure 5. The **e**mission spectra of Mn^{2+}-doped $ZnAl_2O_4$ nanophosphors for various (a) Mn^{2+}-concentrations, Mn^{2+} concentration as a function of maximum intensity and (c) Zn/catalyst mole ratio under 325nm excitation

Figure5 (c) shows the dependence of the emission intensity of $ZnAl_2O_4:Mn^{2+}$ as a function of the Zn/catalyst mole ratio. The results showed there are two emissions bands, which are violet and green, centred at 438 and 693 nm respectively. The mole ration of (Zn/catalyst) = 1.33 had the highest intensity. The results also suggest that the higher the Zn/catalyst mole ratio during synthesis the better the brightness of the phosphor. This is probably due to the catalyst quenching the rate of chemical reaction to allow enough time for the foreign atoms (the activator) to uniformly distribute in the host

lattice matrix. On the other hand, the lesser the Zn/catalyst mole ratio during synthesis the poorer the brightness of the phosphor and this can be due to catalyst saturation, which is essentially speeding up the chemical reaction too much and, as a result, foreign atoms do not get enough time to distribute homogeneously in the host matrix.

4. Conclusion

The green emitting $ZnAl_2O_4:Mn^{2+}$ phosphor with average particle size of 46 nm was successfully prepared by the sol-gel process. It was found that an intermediate phase possibly of a mixture of ZnO and Al_3O_2 is formed at 150 ^{0}C. Minimum annealing temperature required to obtain pure and single phase $ZnAl_2O_4$ is 400 $^\circ$C. The SEM data showed that the samples consist of small crystallites. All expected elements were detected from the EDS spectrum except the Mn due to low mol%. FTIR showed that the number of bands decreases as the sample is heat-treated at higher temperature resulting into pure and ultrafine $ZnAl_2O_4$:0.25% Mn . PL showed that all doped samples with different mol% of manganese and various mole ratio of Zn/catalyst emits in the visible spectrum. Luminescent brightness of $ZnAl_2O_4:Mn^{2+}$ nanophosphor could be enhanced by controlling the Zn/Mn mol% and Zn/catalyst mole ratio. Clear understanding of the basic requirements that regulates the growth conditions that favours either cubic or monoclinic structure and the corresponding effects on the luminescence can be interesting task for further studies.

Acknowledgment

This work is supported by the South African National Research Foundation (NRF) and the research fund of the University of the Free State.

References

1. Zou L, Li F, Xiang X, Evans D.G and Duan X 2006 *Chem Mater* **18** 5852
2. Grabowska H, Zawadzki M and Syper L 2006 *Appl Catal* A **314** 226
3. Tzing W S and Tuan W H 1996 *J. Mater. Sci. Lett.* **15** 1395
4. Mu-Tsun Tsai, Yu-Xiang Chen, Pei-Jane Tsai and Yen-Kai Wang 2010 *Thin Solid Films* **518** e9-e11
5. Sampath S K and Cordaro J F 1998 *J. Am. Ceram. Soc.* **81** 649
6. Tshabalala K G, Cho S –H, Park J –K, Pitale S S, Nagpure I M, Kroo R E, Swart H C and Ntwaeaborwa O M 2011 *J. Alloys Compd.* **509** 10115-10120
7. Keller J T, Agrawal D K and McKinstry H A 1998 *Adv. Ceram. Mater.* **3 420**
8. Van de Laag N J, Snel S G, Magusin P C M M, de With G and Eur J 2004 *Ceram. Soc.* **24** (8) 2417-2424
9. Yuan F L, Hu P, Yin C L, Huang S L and Li J L 2003 *J. Mater. Chem.* **13** 634
10. Vulenzuela M A, Jacobs J P, Bosch P, Reije S, Zapata B and Brongersma H H 1997 *Appl. Catal.* A **148** 315
11. Chen Z, Shi E, Zheng Y, Li W, Wu N and Zhong W 2002 *Mater. Lett.* **56** 601-605
12. Singh V, Natarajan V and Zhu J J 2007 *Opt. Mater.* **29** 1447-1451
13. Adak A K, pathak A and Pramanik P 1998 *J. Mater. Sci Lett.* **17** 559-561
14. Wu Y, Du J, Choy K –L, Hench L L and Guo J 2005 *Thin Solid Films* **472** (1-2) 150-156
15. Alison A, Da Silva, de Souza Goncalves A and Davolos M R 2009 *J. Sol-Gel. Sci. Technol.* **49** 101-105
16. Wei X, Chen D 2006 *Mater. Lett* **60** 823
17. Jamal E M A, Kumar D S and Anantharaman 2011*Bull. Mater. Sci.* **34** 251-259
18. Cullity B D 1978, *1956 Elements of X-ray Diffraction (2nd Ed)*, (Addison Wesley) 285-284
19. Matsui H, Xu C N and Tateyama H 2005 *Appl. Phys. Lett.* **78** 1068
20. Kuang W X, Fan Y N, Yao K W and Chen Y 1998 J. *Solid State Chem.* **140** 354